

Millimeter-Wave Holographic Imaging Algorithm with Amplitude Corrections

Yu-Kun Zhu^{1, 2, *}, Ming-Hui Yang¹, Liang Wu¹, Yun Sun¹, and Xiao-Wei Sun¹

Abstract—Security detection is becoming extremely important with the growing threat of terrorism in recent years. An effective millimeter-wave (mmw) holographic imaging system is presented in this paper, which can be applied in nondestructive detection such as security detection in airport or other public locations. The imaging algorithm is an extension of the work before as it takes the decay of the amplitude with range into account. The experiment result of an imaging system working at 28–33 GHz frequencies indicates good quality of the algorithm.

1. INTRODUCTION AND BACKGROUND

Passenger screening is becoming extremely important with the growing threat of terrorism in recent years [1–8]. Millimeter-wave imaging plays a significant role in passenger screening because it is more effective and safe than other methods of security detection such as metal detector and X-ray scanner. Moreover, millimeter-wave imaging combines the advantages of both optical and microwave systems, high resolution of optical imaging due to the short wavelength and the penetration through most clothing of microwave imaging. In addition, the holographic techniques can be easier to achieve in mmw band than optic-wave as we can get the amplitude and phase of the mmw signal simply.

Millimeter wave imaging can be categorized into passive imaging systems and active imaging systems. There is no illuminating source in passive system [9–11]. It works through recording the intensity of objects. Different electromagnetic strengths are emitted due to the different temperatures, thus scattering information of the target can be obtained. On the other hand, active system transmits mmw signals and receives them reflected by the objects [12–14]. Then the signals are interfered with the transmitting ones, thus both amplitude and phase can be documented.

Because of the advantages of the mmw imaging systems, plenty of positive multi-frequency systems have been designed. Scientists in PNNL translated the holographic algorithm using in far field into near field and got excellent imaging result several years ago. L-3 Communication Company has turned this technique to real product applied in personal security detection. People need to stand about 50 cm away from the scanner when they are screened, which causes that the range distance can be very long since we need two sides of the scanner to obtain information from both the front and back.

Considering all above into account, we present an improved holographic algorithm and realize it as a practical mmw body scanner which can be used in security detection. It is different from the systems presented before. Not only phase but also the amplitude of the signal is delicately dealt with since it has a great influence on the imaging result when the target is close to the scanning plane.

Received 8 May 2016, Accepted 1 July 2016, Scheduled 13 July 2016

* Corresponding author: Yu-Kun Zhu (ykzhu@mail.sim.ac.cn).

¹ Key Laboratory of Terahertz Technology, Shanghai Institute of Microsystem and Information Technology, Shanghai 200050, China.

² University of Chinese Academy of Sciences, Beijing 100049, China.

2. IMAGING ALGORITHM

As shown in Fig. 1, assuming that the reflection coefficient of the target at point (x, y, z) is $g(x, y, z)$ and the scanning plane placed at position $z = Z_s$, the signal obtained at point (x', y', Z_s) is shown in Equation (1), where $k = \omega/c$ and ω is the angular frequency, c the light speed. Here we take the amplitude decay with range into account as the intensity information is important to reconstructing the image when the target is very close to the scanning aperture. More specifically, the signal will decay with the spreading distance increased. The decay caused by different points can be treated the same as when the target is far from the scanning aperture and can be neglected, while it should be considered when the target is close to the transceiver. So the signal $g(x, y, z)$ here is divided by a denominator $((x - x')^2 + (y - y')^2 + (z - z')^2)^2$. The denominator means the decay of the amplitude of the signal after round trip between the antenna and target point. Please pay attention to the difference between the primed and unprimed coordinates. The primed ones take scanning plane as a reference while the unprimed ones are located in the target field.

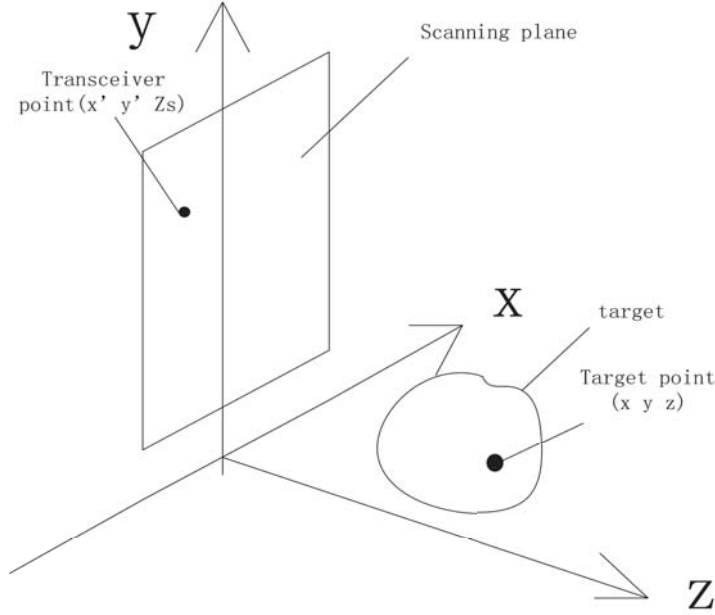


Figure 1. Holographic imaging system configuration.

$$f(x', y', \omega) = \iiint \frac{g(x, y, z)}{((x - x')^2 + (y - y')^2 + (z - Z_s)^2)^2} \times \exp\left(-2jk\sqrt{(x - x')^2 + (y - y')^2 + (z - Z_s)^2}\right) dx dy dz \quad (1)$$

According to the optical knowledge, a sphere wave from one point can be decomposed into infinite plane waves from the same point, which is shown in Equation (2). Then we deal the extra amplitude decay information with Taylor series expansion and truncate it appropriately. After doing all above, we put all the primed symbols out of integration and rearrange to yield Equation (3).

$$\exp\left(-2jk\sqrt{(x - x')^2 + (y - y')^2 + (z - Z_s)^2}\right) = \iint \exp(-jk_{x'}(x - x') - jk_{y'}(y - y') - jk_{z'}(z - Z_s)) dk_{x'} dk_{y'} \quad (2)$$

$$f(x', y', \omega) = FT_{2D}^{-1}[M(x', y') \times G(k_{x'}, k_{y'}, k_z) \exp(jk_z Z_s)] \quad (3)$$

where $M(x', y') = (x'^2 + y'^2 + Z_s^2 + 4x' + 4y' + 4Z_s) / (x'^2 + y'^2 + Z_s^2)^3$, $G(k_x, k_y, k_z)$ is the three-dimension Fourier transform of $g(x, y, z)$. When we calculate the Taylor series of the amplitude terms, the slow changes of x, y, z in $M(x', y')$ compared to other items are neglected because they will have little influence on image reconstruction. Finally, we replace the primed variables with unprimed ones and get the image reconstruction Equation (4).

$$g(x, y, z) = FT_{3D}^{-1} \left\{ FT_{2D} [f(x, y, \omega)] / M(x, y) \times \exp \left(-jZ_s \sqrt{4(\omega/c)^2 - k_x^2 - k_y^2} \right) \right\} \quad (4)$$

In other words, image of the target $g(x, y, z)$ can be calculated through the signal $f(x, y, \omega)$ that we received at the scanning plane. Here we replace k_z with the square according to the principle of $k_x^2 + k_y^2 + k_z^2 = (2k)^2 = 4(\omega/c)^2$.

FT and FT^{-1} here mean the Fourier transform and inverse Fourier transform, respectively. FT_{2D} and FT_{3D} mean two- and three-dimension Fourier transforms, respectively.

3. IMAGING SYSTEM

We produce an imaging system to verify the algorithm presented above. The outline of the mmw holographic imaging system is introduced as follows. Taking the scanning time and the cost of the system into account, we choose to scan a line of transmit and receive antennas array row by row. A diagram of the imaging system is shown in Fig. 2. This system can reconstruct three dimension (3-D) image of the target as wideband frequency signals are recorded. Two levels of SP8T switches are adopted to achieve a row of 64 T/R units.

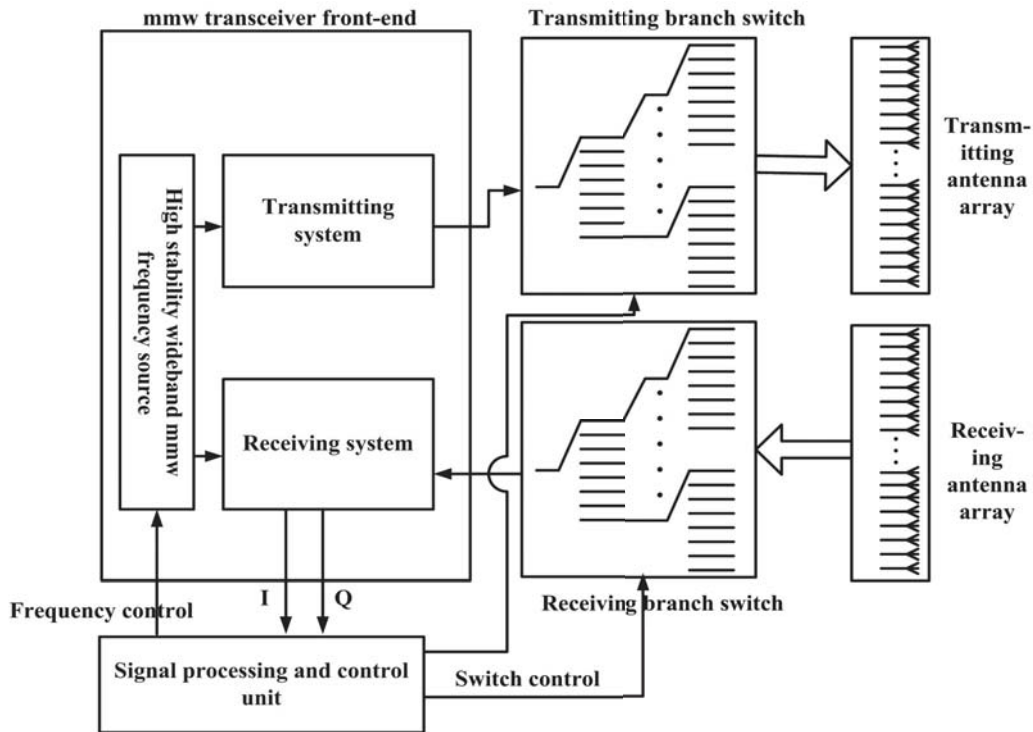


Figure 2. Diagram of the wideband mmw imaging system.

We document both the in-phase and quadrature signals (called I and Q respectively) after mixing the receiving signals with the transmitting ones from mmw oscillators, i.e., both amplitude and phase can be obtained.

According to the diagram, an imaging system is successfully realized in our lab. A prototype of the system is shown in Fig. 3. The distance between antenna elements is chosen to be 6 mm which is a little



Figure 3. The prototype of the wideband mmw imaging system.

larger than half the wavelength 5 mm (ideal distance between elements), since the beam of the antenna is not infinite. Size of the scanning aperture is 76.2 cm * 220 cm, and the scanning time is less than 2 s. There are totally 128 * 380 pixels in the imaging result. The holographic imaging system works at a wide frequency band which is 5 GHz, from 28 GHz to 33 GHz.

4. IMAGING RESULT

With the system introduced before, simulation has been implemented. The result proves great performance of the holographic imaging algorithm.

Figure 4 shows different reconstruction results of the ideal point placed 30 cm away from the scanning aperture using (b) traditional [15] and (a) improved algorithm that we present in this paper, respectively.

As shown in the simulation results, the reconstruct image of the ideal point with improved algorithm presented in this paper decreases the side lobe compared with the traditional one.

The following imaging results of different targets carried by different persons are obtained with the system mentioned above, and the person with targets stands 30 cm away from the transceiver antenna.

Figure 5 shows a metal toy gun with taped outside, a bottle of water and a cellphone which are our model targets. Fig. 6 shows (a) the optical and reconstructed image of a person with the gun in his pant pocket and a bottle of water in his hands, and (b) the optical and reconstructed image of a person with a cell phone in a pant pocket and a bottle of water in the other pocket. Fig. 7 shows the comparison of the reconstructed imaging results applying the algorithm with traditional and improved algorithms.

All the imaging results posted above are the front view of the model because we only put the targets in the front of the models. Results in Fig. 6 show great performance of our algorithm and the holographic imaging system. As shown in Fig. 7, when the target is close to the scanning aperture, obviously, the reconstructed image with improved algorithm gives a better performance since it is considered that the amplitude decay varies greatly between different transceiver points and target points. That is to say the decrease of side lobe of the point gives better imaging result which we can see from the comparison between the reconstruction images using traditional algorithm and the one that we present.

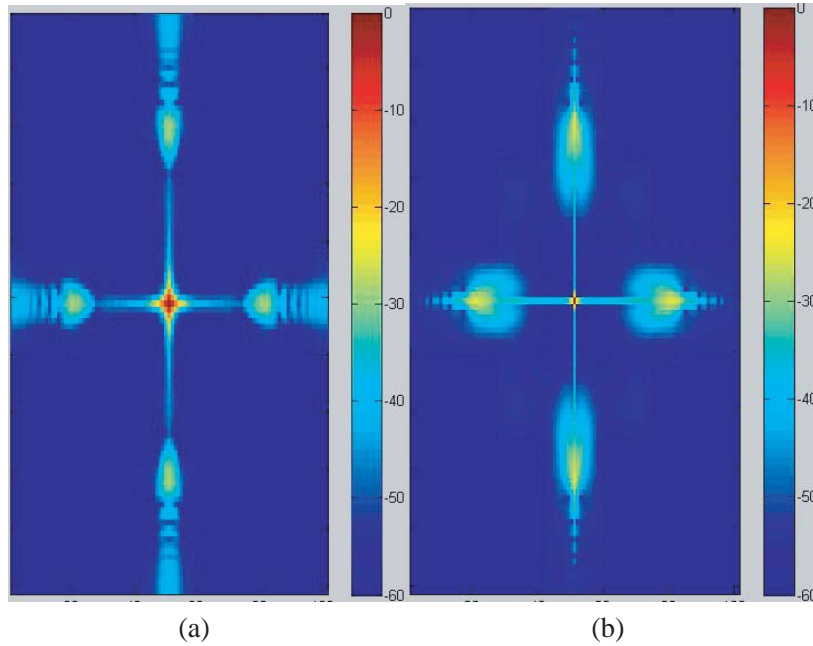


Figure 4. Results of ideal point using (b) traditional and (a) improved algorithm.

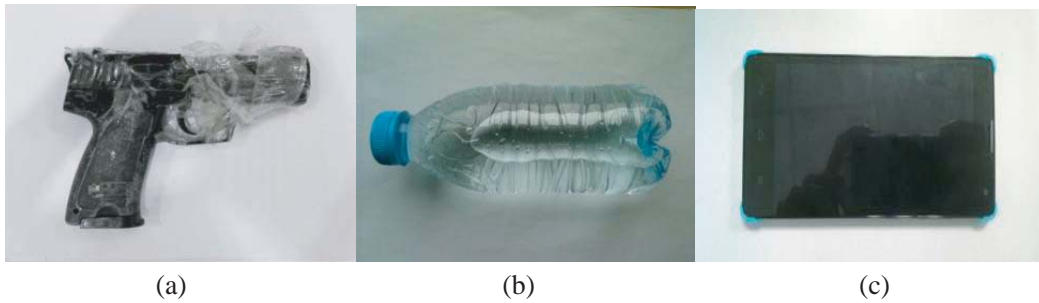


Figure 5. (a) A taped metal toy gun, (b) a bottle of water, (c) a cellphone.

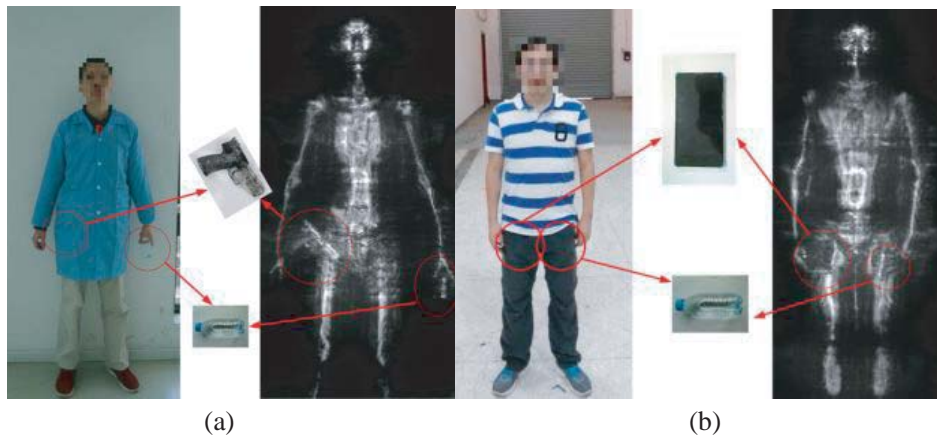


Figure 6. (a) Imaging result of a man with a gun and a bottle of water, (b) imaging result of a person with cell phone and a bottle of water.

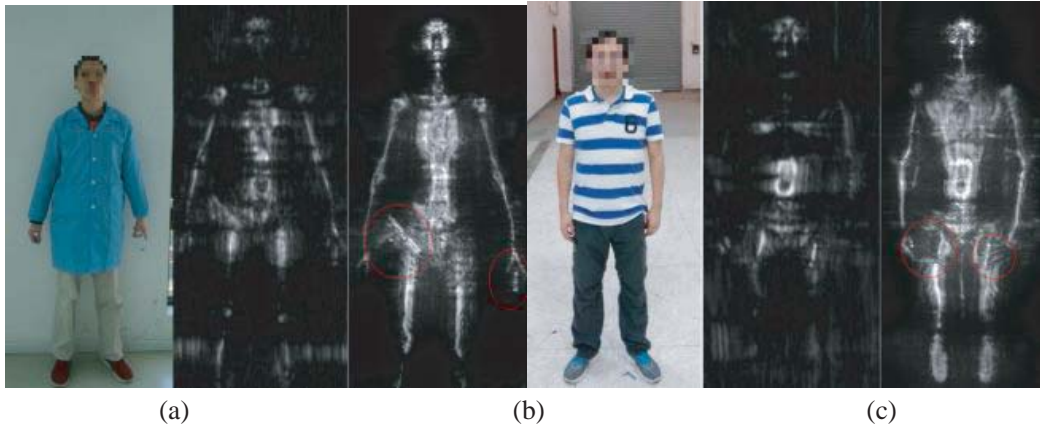


Figure 7. Comparisons of the (a) optical images reconstruct imaging results applying the algorithm with (c) improved and (b) traditional the corrections presented in this article.

We may notice that this algorithm will decrease the side lobe of the point, however, also cause worse spread of the ideal point, which is a problem that we need to solve next.

5. CONCLUSIONS

In conclusion, a high resolution wide-band millimeter-wave active imaging system is implemented. The working frequency band of this system is from 28 GHz to 33 GHz. The imaging results of different persons with several targets are presented. Improvements of the algorithm compared with the original one are obvious, which indicates that our system and algorithm are feasible and effective. However, there are also some drawbacks in the imaging system, which only gives the outline of the target without the material chemical properties. So the indicator can only rely on the shape of the target to distinguish if the object is safe or not. Auto target detection should be added in the future.

REFERENCES

1. Brooker, G., R. Hennessey, M. Bishop, et al., "Millimeter wave 3D imaging for industrial applications," *International Conference on Wireless Broadband and Ultra Wideband Communications*, 27, 2007.
2. Chen, J., Y. Li, J. Wang, Y. Li, and Y. Zhang, "An accurate imaging algorithm for millimeter wave synthetic aperture imaging radiometer in near-field," *Progress In Electromagnetics Research*, Vol. 141, 517–535, 2013.
3. Gonzalez-Valdes, B., Y. Alvarez-Lopez, J. A. Martinez-Lorenzo, F. Las Heras Andres, and C. M. Rappaport, "On the use of improved imaging techniques for the development of a multistatic three-dimensional millimeter-wave portal for personnel screening," *Progress In Electromagnetics Research*, Vol. 138, 83–98, 2013.
4. Demirci, S., H. Cetinkaya, E. Yigit, C. Ozdemir, and A. A. Vertiy, "A study on millimeter-wave imaging of concealed objects: Application using back-projection algorithm," *Progress In Electromagnetics Research*, Vol. 128, 457–477, 2012.
5. Appleby, R. and H. B. Wallace, "Standoff detection of weapons and contraband in the 100 GHz to 1 THz region," *IEEE Transactions on Antennas and Propagation*, Vol. 55, No. 11, 2044–2056, 2007.
6. Zhang, L., Y. Hao, C. G. Parini, and J. Dupuy, "An experimental millimetre wave imaging system," *Loughborough Antenna and Propagation Conf. (LAPC '08)*, Loughborough, UK, March 17–18, 2008.

7. Bjarnason, J. E., T. L. J. Chan, A. W. M. Lee, M. A. Celis, and E. R. Brown, "Millimeter-wave, terahertz, and mid-infrared transmission through common clothing," *Applied Physics Letters*, Vol. 85, No. 4, 519, 2004.
8. Guan, F.-H., M.-H. Yang, J. Xu, et al., "Miniaturization Ka-band receiver used for passive millimeter wave imaging," *J. Infrared Millim. Waves*, Vol. 29, No. 4, 241–244, 2010.
9. Appleby, R., "Passive millimetre wave imaging and security," *European Radar Conference*, Amsterdam, Netherlands, 275–278, 2004.
10. Zhang, Y.-D., Y.-S. Jiang, Y.-T. He, et al., "Passive millimeter-wave imaging using photonic processing technology," *J. Infrared Millim. Waves*, Vol. 30, No. 6, 551–555, 2011.
11. Shi, X. and M. H. Yang, "Development of passive millimeter wave imaging for concealed weapon detection indoors," *Microwave and Optical Technology Letters*, Vol. 25, No. 7, 1701–1706, 2014.
12. Sheen, D. M., D. L. McMakin, and T. E. Hall, "Cylindrical millimeter-wave imaging technique and applications," *Proceedings of SPIE*, Vol. 6211, 2006.
13. McMakin, D. L., D. M. Sheen, J. W. Griffin, and W. M. Lechelt, "Extremely high-frequency holographic radar imaging of personnel and mail," *Proceedings of SPIE*, Vol. 6201, 2006.
14. Sheen, D. M., D. L. McMakin, and T. E. Hall, "Near field imaging at microwave and millimeter wave frequencies," *IEEE/MTT-S International*, 169–1696, 2007.
15. Sheen, D. M., D. L. McMakin, and T. E. Hall, "Three-dimensional millimeter-wave imaging for concealed weapon detection," *IEEE Transactions on Microwave Theory and Techniques*, Vol. 49, No. 9, 1581–1592, 2001.